Pure & Appl. Chem., Vol. 69, No. 8, pp. 1725–1740, 1997.
Printed in Great Britain.

INTERNATIONAL UNION OF PURE
AND APPLIED CHEMISTRY

MACROMOLECULAR DIVISION
WORKING PARTY ON STRUCTURE AND PROPERTIES OF COMMERCIAL POLYMERS*

CHARACTERIZATION OF FINITE LENGTH COMPOSITES: PART III. STUDIES ON THIN SECTIONS EXTRACTED FROM MOLDINGS (WAFERS)

(Technical Report)

The authors and contributing members dedicate this paper to their colleague and friend, Professor Gerhard Zachmann

Prepared for publication by

A. CERVENKA[1] AND P. S. ALLAN[2]

[1]Shell Research B.V., Koninklijke/Shell Laboratorium, Amsterdam, Netherlands
[2]Brunel University, The Wolfson Centre for Materials Processing, Uxbridge, Middlesex, UK

*Membership of the Working Party during the preparation of this report (1996–97) was as follows:

D. R. Moore (UK); A. Cervenka (Netherlands); H. Motz (FRG); P. S. Allan (UK); G. Ajroldi (Italy); F. H. J. Mauer (Sweden); B. Gunessin (USA).

Characterization of finite fibre-length composites: Part III: Studies on thin sections extracted from moldings (wafers) (Technical Report)

Abstract: Through-thickness aspects of composites are studied by means of structural investigations and mechanical testing of thin 'wafers' machined from molded specimens. Two injection molding regimes, namely the Dynamic and Static mode, have been used to induce different fibre orientations in polypropylene (PP) reinforced with glass (g) and polyamide (PA) reinforced with carbon (c). Novel experimental techniques such as the 'rebound technique', uniaxial compressive yield and flexural testing of circular discs have been used for evaluation of longitudinal and transverse properties.

A strong anisotropy of properties in composite moldings is governed by the spatial fibre orientation. This depends on both the matrix and the processing conditions used with the system PP/g being more regularly structured (skin/core morphology) than PA/c.

A satisfactory agreement in the area a) structure/performance and b) experiment/theory has been achieved.

1. INTRODUCTION

IUPAC Working Party 4.2.1 (Structure and Properties of Commercial Polymers) has been involved in a series of studies addressing generic behaviour of the composites based on a thermoplastic matrix and reinforced with discontinuous (finite length) fibres. The generic aspects studied were the type of the matrix, the nature of the reinforcement, fibre length and the effect of processing conditions used for injection molding which have been overviewed in a summary paper by Cervenka and Allan (ref. 1).The studies were geared towards establishing structure/property relationships and these are reported in other parts of the series. Whilst properties of the composite moldings are overviewed by Glas *et al* (ref. 2), theoretical rationalisation of observations concerning performance aspects is contained in the contribution by Moore *et al* (ref. 3) and structural aspects are covered by the study of von Bradsky *et al* (ref. 4).

On the basis of these studies, the composite performance has been concluded to be chiefly a manifestation of structure formed during a particular injection moldings step rather than a simple material response with respect to the type of constituents and their relative concentrations.

The aim of this paper is to supplement the information obtained by investigating composite moldings as reported in refs. 1–4 and to provide a more detailed assessment of the composite anisotropy by studying composites that have been cut into thin 'wafers'. Variation of the structure and mechanical performance in the thickness direction and their relation to the spatial orientation of fibres are here the key issues.

The following laboratories participated in this study:

(a) Ausimont S.p.a., Bollate, Italy
(b) BASF, Polymer Research Division, Ludwigshafen, Germany
(c) DSM, Geleen, The Netherlands
(d) Shell Research B.V., Arnhem, The Netherlands
(e) ICI plc, Materials Centre, Wilton, United Kingdom
(f) Huls AG, Marl, Germany

2. EXPERIMENTAL

2.1 Studied composites

The project has addressed finite-length fibre composites of the Verton type based on two matrices (polypropylene - PP and polyamide - PA), three reinforcements (glass - g, carbon - c and Kevlar - k) with the feedstock for the injection molding available at two lengths: Initial fibre length L_i = 5 and 10 mm. Two

injection molding regimes were used to fabricate test specimens: The Dynamic mode based on the 'Multiple Live-Feed' (MLF) approach that causes preferential fibre orientation in the melt flow direction and the Static mode being the classical injection molding method. These two processing routes and the codes used to identify composite types are detailed in ref. 1.

The study reported in this paper concentrates on the behaviour of PP/g and PA/c composites only.

2.2 Specimen preparation

Deduction of composite properties from those of thin sections in the form of either wafers or discs requires a number of assumptions to be satisfied. These are:

(i) The plaques molded under identical processing conditions have the same properties in terms of the fibre spatial distribution, crystallinity, etc.

(ii) There is a symmetry in the properties with respect to the central planes running in the molding direction.

(iii) Mechanical properties of wafers are not influenced by cutting fibres with out-of-plane orientations.

(iv) Mechanical machining does not influence matrix properties and

(v) Elastic properties of the cut wafers are unaffected by relieving residual stresses.

With this in mind, the cutting plan for the wafer preparation was designed (Fig. 1) by laboratory a. Four plaques were required to prepare the complete set of wafers. The cutting operation itself, also carried out by laboratory a, involved (i) making of prismatic bars (80 x 10 mm x plaque thickness) with their major axis either parallel with (specimens coded A-C') or perpendicular to (specimens coded X-Z') the injection direction, (ii) slicing them (circular saw 1 mm thick of 50 mm diameter with 27 teeth, linear speed of 70 mm/min, 850 revolutions/min) and (iii) polishing the surfaces with sand paper.

Whilst the wafer preparation was trouble-free for the PP/g composite, problems were encountered with the PA/c system. Here strong wear required frequent changes of the tool and also the resulting wafer cross-section was not always constant.

Discs, 80 mm diameter and 3 mm thick, were obtained by removing the excess of the material on a lathe so that only one disc was prepared from a given plaque. Three discs were obtained for the PP/g 10 composite for each molding condition. Their relative positions are indicated in Fig. 2. The machining was done using a Vidia one edge tool rotating at 500 rpm with a linear speed of 25 mm/min and cooling the material with compressed air. Preparation was completed again by polishing with sandpaper.

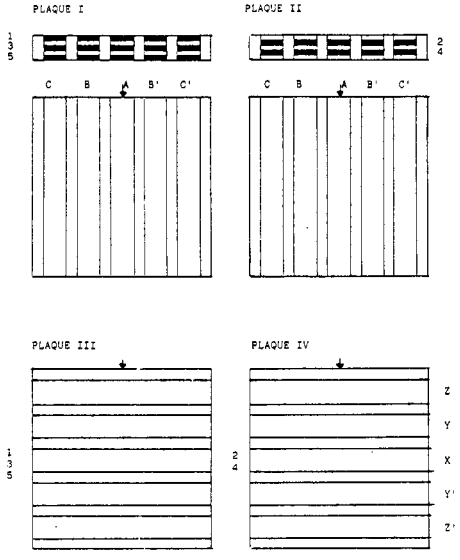

Fig. 1 Wafer preparation: Cutting plan and specimen identification.

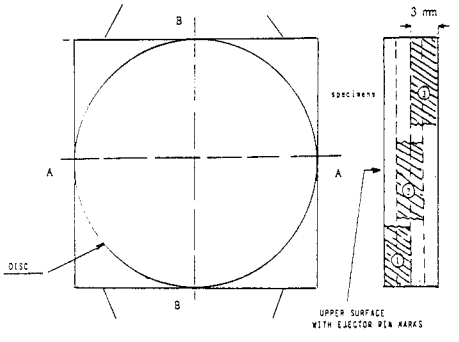

Fig. 2 Disc preparation and specimen coding

2.3 Investigation methods

2.31 Structural studies

X-ray analysis: Wafers and discs were analysed (laboratory f) by underlining a studied material with an X-ray sensitive film and enlarging the negative image by a factor of two.

SEM analysis: Fracture surfaces of wafers after tensile testing were examined by laboratory f using a Joel model 840 Scanning Electron Microscope and coating specimens with Au/Pd alloy.

2.32 Mechanical testing

A number of techniques were used to characterise wafers and discs for their tensile, flexural, creep and compressive behaviour.

The modulus of wafers was determined by means of the rebound technique which makes use of an instrumented impact pendulum (ref. 5) deforming specimens in the tensile and flexural (3-point bending) mode. Two specimen configurations were used in order to reveal anisotropy: i) edgewise configuration with the force exerted on the longer specimen edge and ii) flatwise configuration. Doing the measurement in the flatwise mode twice by applying the load to either flat surface, additional information on fibre distribution through the specimen thickness was generated.

Briefly, the rebound technique investigates material response to a hammer dropped from an angle between 2 and 3°. The modulus is derived from a harmonic time dependence using the general equation reading:

$$E'(\omega) = MK\left(\frac{\pi}{t_o}\right)^2 \tag{1}$$

with K being a shape factor depending on the experimental approach used. Analytical expressions leading to K factors are given in Table 1 while Table 2 defines the symbols used.

Table 1 Analytical expressions for the K factors

Technique	K
tensile impact	$L_o/(AD)$
3-point bending	$L_o^3 T/(48I)$
impact of a clamped disc	$0.75a^2(3+\nu)(1-\nu)/[\pi h^3]$

Two different pendulum machines were used: for the tensile and 3-point bending experiments a Zwick 5101 (frame stiffness k_m=10kN/mm). The other one used for testing of discs was a modified Vaschetti and Grosso pendulum (k_m= 8kN/mm). Here a circular clamp (80 mm diameter) was used and the dart radius was 10 mm.

Low speed flexural stiffness of discs as a function of the angle between applied stress and mold filling direction during specimen preparation was measured by laboratory a.. The method and equations reported by Stephenson (ref. 7) were used. Discs were tested in the 3-point bending mode (Fig. 3) by means of the Instron model 1185 machine at a testing speed of 0.033 mm/s and working with the span of 65 mm. The maximum deflection was 0.5 mm. The modulus was calculated from:

$$E = (1-\nu^2)\frac{3P}{h^3\delta}f(R,B)$$

with (2)

$$f(R,B) = [R-B]\{-2R + 1.5(2RB - B^2)^{1/2}\} + \frac{3R^2 - 4RB + 2B^2}{2}\arcsin\frac{R-B}{R}$$

Compressive properties at the ambient temperature were measured by laboratory e. Thin sections were fabricated by using a rotary cutter on a milling machine. Fig. 4 shows the range of thicknesses used and

Table 2 Meaning of the symbols used

A	cross-sectional area
a	radius of the support
B	R-[L_O/2]
b	side of the specimen square
D	experimentally determined constant 0.89 accounting for the Saint–Venant effect (ref. 6)
$E'(\omega)$	the real part of the Young's modulus at an angular frequency ω
h	specimen thickness
I	moment of inertia = $hW^3/12$
L_O	specimen span
M	mass of the hammer
P	measured load
K	a shape factor depending on the testing method
R	radius of the circular specimen
T	shear correction = $(1+2.85[W/L_O]^2 - 0.84[W/L_O]^3$
t_O	rebound time, i.e. half-period of the sinusoidal response; inversely proportional to the specimen compliance when damping is small. The measured compliance C has to be corrected for the machine compliance C_m when necessary.
W	specimen width
δ	deflection
μ	friction coefficient for the specimen/platen contact
ν	lateral contraction ratio
σ_A	applied compressive stress
σ_T	compressive stress in the specimen

the specimen locations. Yield strength under uniaxial compression was measured at a speed of 1.67 μm/s using an Instron 6025 testing machine. Since uniaxial compression of thin plaques results in considerable frictional forces between the specimen surfaces and the compression platens, this undesired effect was minimised by lubricating specimen surfaces and its contribution to measured compressive stresses was eliminated by working with different thickness/surface area ratios. Side dimensions of square specimens were 7, 7.5 and 10 mm. Deformation of slender specimens of this type is described by:

$$\sigma_A = \sigma_T[1+\frac{\mu b}{4h}] \tag{3}$$

Thus the plot of σ_A versus b/4h is a straight line yielding the material property σ_T as the intercept at the zero value of the argument.

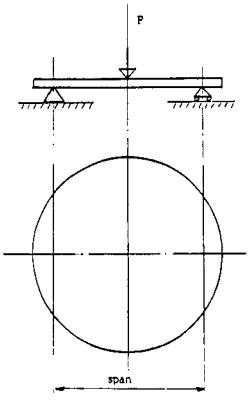

Fig. 3 Flexural testing of thin discs

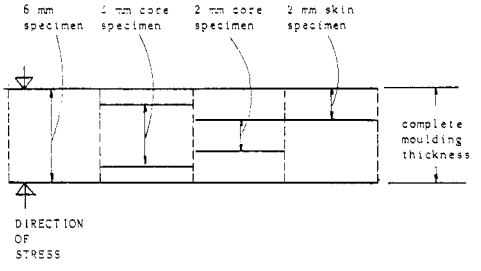

Fig. 4 Samples for uniaxial compression - position and coding

The relaxation moduli (10 s) in the longitudinal and transverse directions of bars prepared from the PP/g moldings were determined by laboratory c. The moldings were sawn into bars as illustrated in Fig. 5. Their approximate width was 5.9 mm. The stiffness was measured by relaxation experiments (1000 s duration) carried out at 25 °C and straining to 0.2%. Deformation was imposed within 0.5 s. All experiments were done on a ZWICK 1474 closed loop controlled tensile testing machine. Forces were measured with a 10 kN force transducer (Hottinger Baldwin U2A) that had an accuracy of 0.1 N. The measured force was typically 300 N. A strain sensor (ZWICK WNR 93031) clamped on a 50 mm gauge sample was used to monitor the strain with an accuracy of 0.01 mm. The temperature was kept constant within ± 0.2 °C in a temperature controlled oven.

Finally, ultimate tensile properties of the PA/carbon wafers, namely the strength and the elongation, were measured by laboratory b. Working at ambient temperature and a testing speed of 8.33×10^{-2} mm/s, thin specimens were deformed by means of a Mini-mat tester with a gauge length of 10 mm.

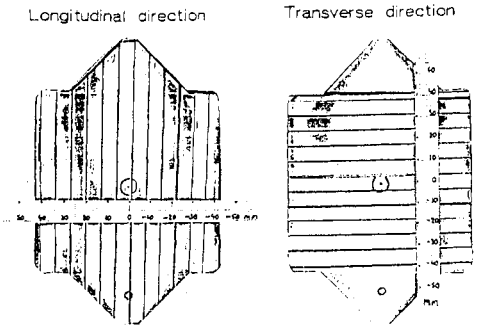

Fig. 5 Fabrication of bars for creep measurements (illustration for moldings from the DYNAMIC mode).

3. RESULTS

3.1 composite structure

Structural techniques - X-ray radiography and the scanning electron microscopy of fractured surfaces - employed for the PP/g and PA/c composites clearly signal that different fibre orientations have been attained as a result of the processing conditions and the matrix/reinforcement partnership. Defining the molding to be a three-dimensional structure of length D, width W and thickness Z, any position in the test coupon can be identified by means of three coordinates, namely $-D/2<x<D/2$, $-W/2<y<W/2$ and $-Z/2<z<Z/2$, with the spatial fibre distributions conforming to the following patterns:

Concentrating firstly on the PP/g system, X-ray radiography used for investigation of rectangular wafers and circular discs (laboratory f) shows that the Dynamic processing results in a more pronounced orientation in the x-direction, cf. ref. 1) and leads to a laminated structure with the 'skin' regions near the mold surfaces $Z/2$ and $-Z/2$ and the 'core' region alongside the mid-thickness plane $z=0$. Although cutting of moldings into only 5 wafers does not allow their proportions to be quantified (this information is reported in ref. 4), the regions exhibit distinctly different fibre orientations: The 'skin' fibres appear to be parallel with and the 'core' fibres perpendicular to the major axis x of the molding. In addition, whilst wafers cut in the longitudinal direction indicate very little variation in the fibre orientation in the x direction, transverse wafers reflect a gradual change in the fibre orientation in the y-direction with a more perfect alignment along the x-axis for $y \rightarrow |W/2|$. Thus the wafers associated with $z \rightarrow |Z/2|$ and $y \rightarrow |W/2|$ represent the regions where the maximum longitudinal characteristics ought to be obtained. Structural investigations of circular discs broadly confirm this conclusion.

As to the Static processing (classical injection molding), glass fibres in the polypropylene matrix appear to approximate to a random distribution in the 'skin' regions with a certain tendency to longitudinal (x-axis) orientation for $y \rightarrow |W/2|$. The 'core' region, on the other hand, is preferentially reinforced by fibres transversely oriented to the melt flow. Thus the wafer cut along the x-axis and extracted from the region $z \rightarrow 0$ and $y \rightarrow 0$ ought to yield the transverse laminar response.

A supporting observation of wafer anisotropy has been made from distortion of the wafer strips after cutting, i.e. the phenomenon associated with frozen-in thermal stresses: Whilst the longitudinal strips prepared by cutting moldings manufactured by the Dynamic mode and the transverse strips associated with the Static mode remained essentially parallel (a pack of cards), the other pair completing the 2x2 'processing mode/cutting direction' matrix deformed. Here the transverse wafers extracted from the 'skin' ($z \rightarrow |Z/2|$) regions of the Dynamic mode moldings and the longitudinal wafers representing the 'core' ($z \rightarrow 0$) region of the Static mode moldings both bowed outwards.

An entirely different spatial fibre distribution has been found for the PA/c composite: Irrespective of the processing mode, the SEM fractography (laboratory b) does not indicate the presence of the expected 'skin/core' morphology when results are scrutinised in the z-direction. The fibre orientation is systematically seen to be three-dimensional, however with the processing mode dictating the preferred fibre orientation: The Dynamic processing mode tends to orient fibres in the direction parallel to the mold fill direction (fibre bristles protruding from fracture surfaces of longitudinal specimens, fibre imprints after debonding from the matrix during the failure of transverse specimens). The same fractographical reasoning is used for concluding that the Static processing is associated with the preferred fibre orientation perpendicular to the melt flow. Analysing the fractured surfaces in the x- and y-directions, the fibre orientation is very heterogeneous (more pronounced for the Dynamic mode processing, often associated with matrix rich regions) with respect to the relevant coordinate in a wafer plane. Acknowledging fully the existence of anisotropy in moldings, the major theme in fibre distribution is that of 'streaky' patterns spreading randomly in the plane under investigation. These structural aspects are a consequence of an uneven mold filling as documented in ref. 1 and in line with i) the map of in- and out-of-plane fibre inclinations generated by means of the image analysis (ref. 4), ii) unusually large scatter in mean tensile properties on moldings as reported by participating laboratories (ref. 2), iii) high standard deviations on a mean value reported by a given laboratory (ref. 2) and iv) ill-defined property (stiffness and strength) profiles assembled from data generated for wafers. Concerning the fibre/matrix adhesion, qualitatively the Static mode appears to have resulted in stronger interfacing as judged by the amount of polymer deposited on fibres and an average fibre pull-out length.

No attempt has been made to analyse wafers for their distributions in fibre length.

3.2 Mechanical performance

3.21 System polyamide/carbon fibre

Recalling that this composite type involved 10 mm long pellets as the feed stock only, data on the rebound moduli measured by laboratory a through the plaque thickness are shown in Fig. 6 for the Dynamic molding and in Fig. 7 for the Static mode. The specimen position is defined in Fig. 1.

For the Dynamic molding (Fig. 6), anisotropy in the thickness direction is practically absent for the Z, Y and X specimens, whilst some distribution in stiffnesses is observed for the Y' and Z' position (close to the lower injection point). In contrast to these findings in the direction transverse to the flow, results obtained for the longitudinal specimens (A, B, C, B' and C') manufactured by the identical processing route show a very distinct pattern: One half of the plaque (B' and C') shows different properties from the other half (B and C) with the latter (A, B and C) exhibiting maximum stiffness near the surface.

As to the Static injection molding (Fig. 7), different modulus profiles are encountered with a more regular distribution of moduli through thickness for the specimens in both (longitudinal and transverse) principal directions. Here the highest moduli are found at the surface in the longitudinal direction and in the core of the transverse direction. However, the lowest moduli in the transverse direction are higher than those associated with the core region contained in the longitudinal specimens.

Comparing now the two processing routes used for fabricating this composite type, the Dynamic processing seems to lead to a higher anisotropy in the injection (longitudinal) direction in terms of through-thickness moduli than the static method. The opposite is true for the transverse direction where the Static injection molding leads to a more pronounced anisotropy in terms of the through-thickness modulus variation.

Laboratory b determined the strength and elongation at break of composite wafers by a mini-mat tester. Ultimate elongations were significantly below 1% and the fractures were typically brittle. All relative strength data on the wafers for the transverse and longitudinal directions are given in Figs. 8 (Dynamic molding) and 9 (Static molding). The strength data have been normalised on the value measured for specimen X-3 (z and $x \rightarrow 0$) extracted from the molding manufactured by the dynamic mode. In very broad terms, strength data for the wafers show similar through-thickness patterns to those already discussed for the moduli. Definition of strength profiles is however hampered by a larger scatter and also the restricted amount of experimental information.

3.22 System polypropylene/glass fibre

Elastic moduli measured by laboratory a on two sets of specimens in both the 'flatwise' and ' edgewise' directions by the rebound technique are given in Figs. 10 and 11. Fig 10 portrays the situation for the longitudinal moduli (specimens coded C, B A, B' and C') and Fig. 11 provides the same information for the transverse moduli (wafers Z, Y, X, Y' and Z').

The most striking stiffness profile is that exhibited by the longitudinal modulus for the Static mode (Fig. 10): A strong minimum is noticed at the centre part of the plaque and maximum values of stiffnesses are measured near the surfaces. The profiles do not change with the y-coordinate. The maximum values for the Static mode of processing attain, however, a lower value than that determined, in the same plaque $z \rightarrow |Z/2|$ region, for the composites manufactured by means of Dynamic injection molding.

A more complex pattern of longitudinal moduli has been found for the Dynamic mode (Fig. 10). Here the central region ($z \sim 0$) is associated with a stiffness appreciably lower than that of the other four wafers which fall within a relatively broad band and do not conform to a clear trend. The gap between the band median and the minimum value is furthermore seen to vary with the wafer position in the plaque (y-dependence) and reaches its maximum at $y \sim 0$.

Transverse moduli of the composites manufactured by the Static injection molding (Fig. 11) appear to yield an ill defined maximum at $z \rightarrow 0$ which is an increasing function of the x-coordinate. In the case of the

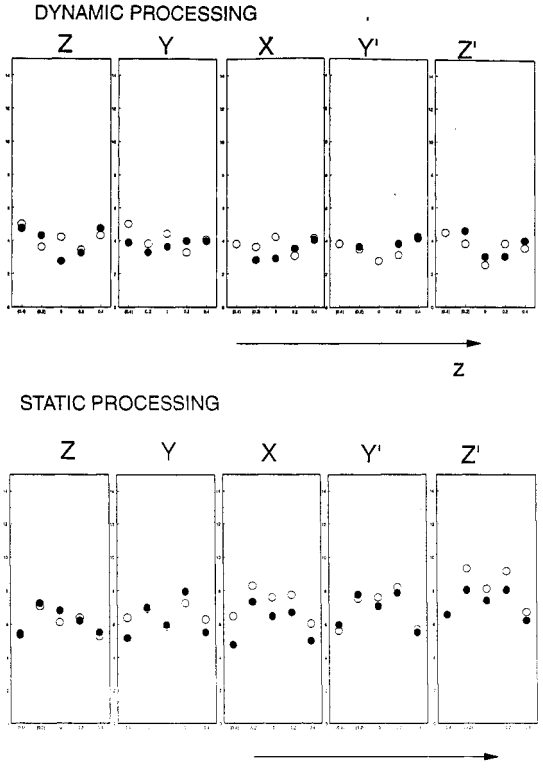

Fig. 6 Stiffness profiles (rebound modulus [GPa]): Filled in circles represent edgewise measurements, open circles illustrate the flatwise configuration; wafer coding in letters as shown in Fig. 1. System: PA/c - 10 DYNAMIC.

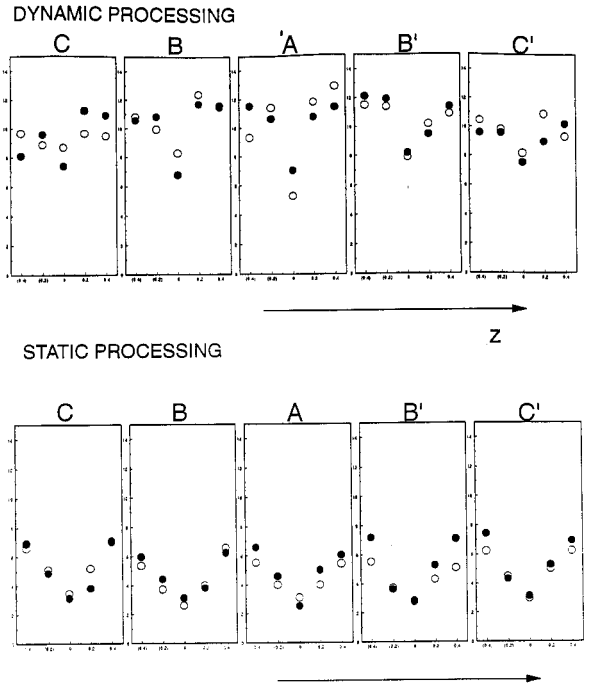

Fig. 7 Stiffness profiles (rebound moduli [GPa]); symbols as in Fig. 6. System: PA/c - 10 STATIC.

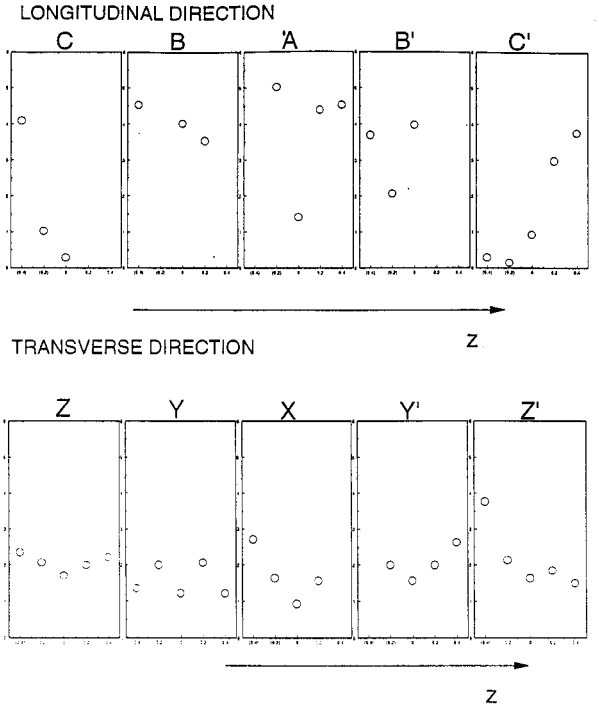

Fig. 8 Relative (data normalised on the result for X-3) strength profiles. System: PA/c - 10 DYNAMIC.

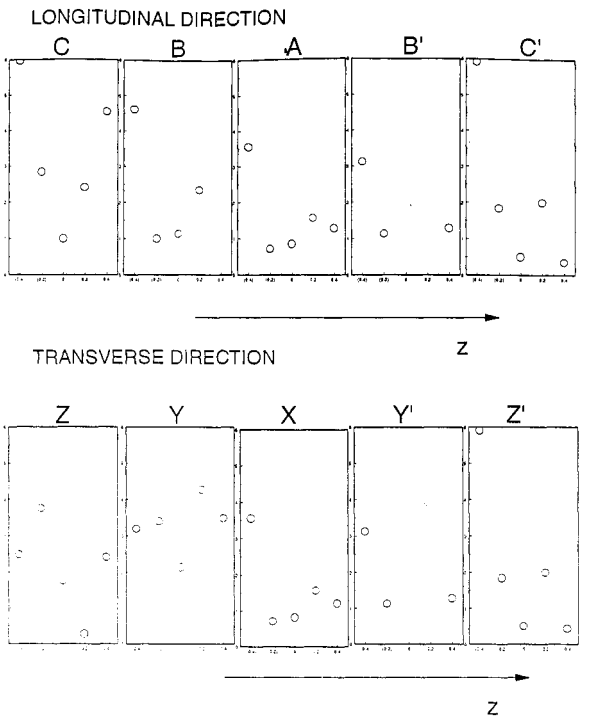

Fig. 9 Relative (data normalised on the result for X-3) strength profiles. System: PA/c - 10 STATIC.

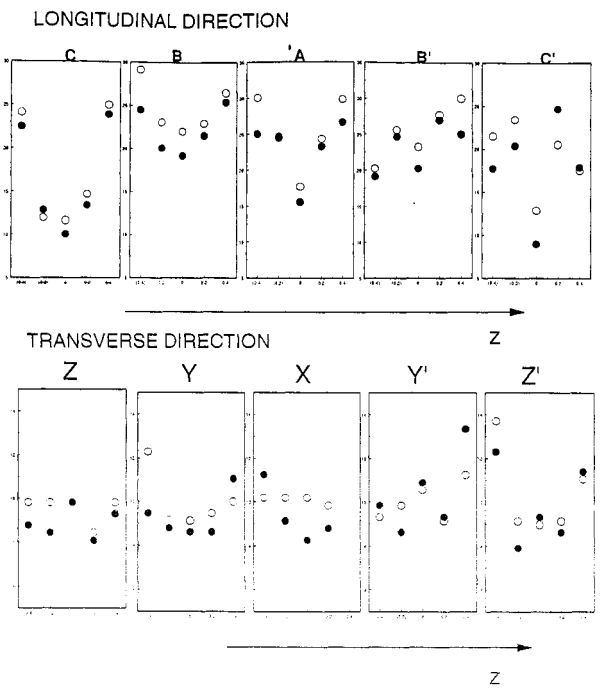

Fig. 10 Longitudinal stiffness profiles for PP/g - 10 composites; Set-1 on open and Set-2 in filled-in circles.

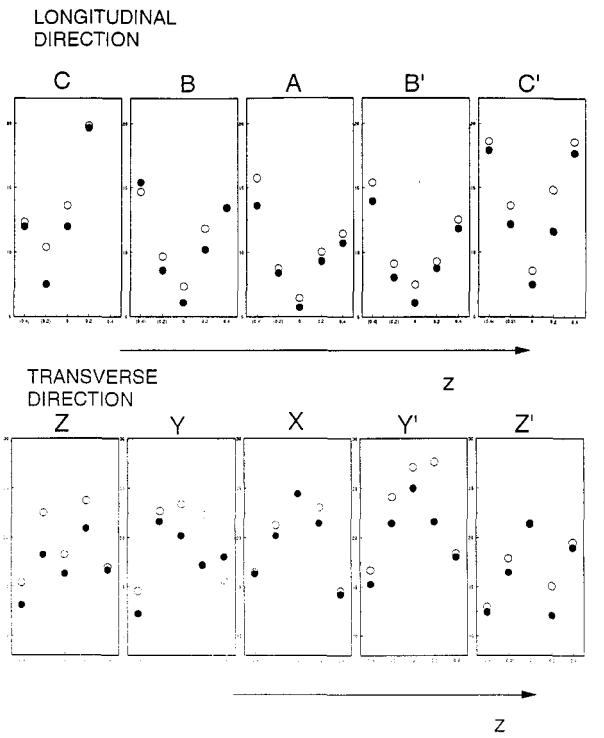

Fig. 11 Transverse stiffness profiles for PP/g - 10 composites; Symbols as in Fig. 10.

Dynamic molding, transverse moduli conform to a simple profile independent of the wafer position in the original plaque. Their values are generally low.

Although the reported results deal with characterization of the structure, material characteristics of the building block - PP/g lamina - can be extracted on the basis of the micromechanical modelling. Defining that composite constituents i are isotropic materials characterised by two elastic constants, namely by a

Young's modulus E_i and a lateral contraction ν_i, calculation based on the equations given in another of our communications (ref. 3) and utilising experimentally determined (ref. 4) information on the reinforcement (concentration v_f, fibre length distributions n[L] generated by three laboratories) allow the glass/polypropylene partnership to be quantified in the material sense. With the input E_m = 1.7 GPa, E_f = 72 GPa, ν_m=0.35, v_f=0.2 and ν_f=0.187, the longitudinal modulus of the lamina (lamina implies perfect fibre alignment) is calculated to be between 11.84 and 13.66 GPa, and the corresponding transverse value is estimated to be about 2.45 GPa. In the light of this calculation, the surface region ($z \rightarrow |Z/2|$) of the moldings manufactured by the Dynamic injection and the core region ($z \rightarrow 0$) of the moldings made by the Static injection appear to be true laminae. Thus the micromechanical treatment verifies the conclusion drawn from the performance testing, namely that molded structures involve regions with a high level of fibre orientation.

The outcome of the stiffness characterization of wafers by the rebound technique has been further reinforced by laboratory a which determined three-point flexural moduli of sliced circular discs as a function of the testing direction relative to that of melt injection. Results are given in Fig. 12. As this type of measurement averages elastic constants over a plane, stiffnesses measured by this technique are expected to be bounded by the longitudinal and transverse stiffnesses determined for the wafers. Without placing too much importance on the absolute values measured, the data reported in Fig. 12 confirm the large anisotropy between longitudinal and transverse direction for the Dynamic processing due to preferential fibre alignment in the molding direction. For the Static injection, the overall anisotropy seems to be lower with the highest fibre orientation in the central part and perpendicular to the melt flow direction.

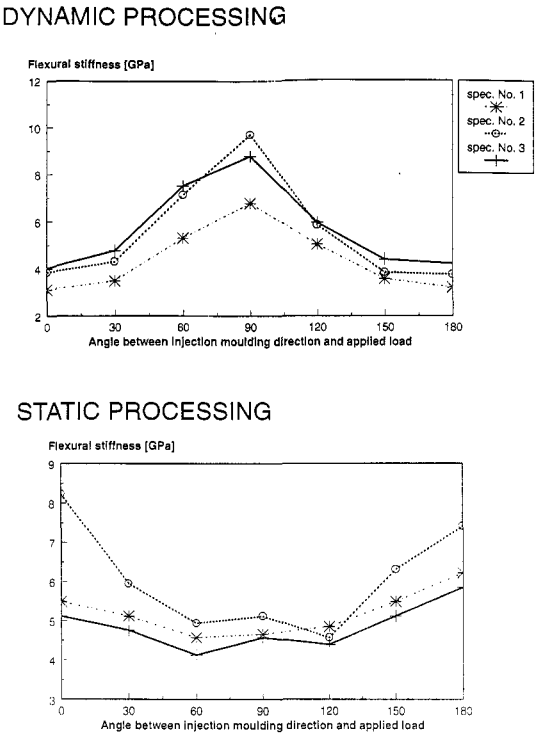

Fig. 12 Angular stiffness dependence determined by flexing disc: System: PP/g - 5.

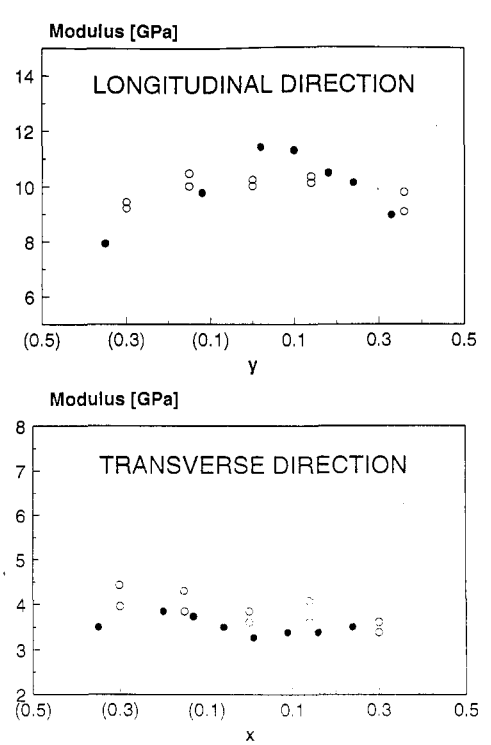

Fig. 13 Creep moduli profile for PP/g - 10 DYNAMIC

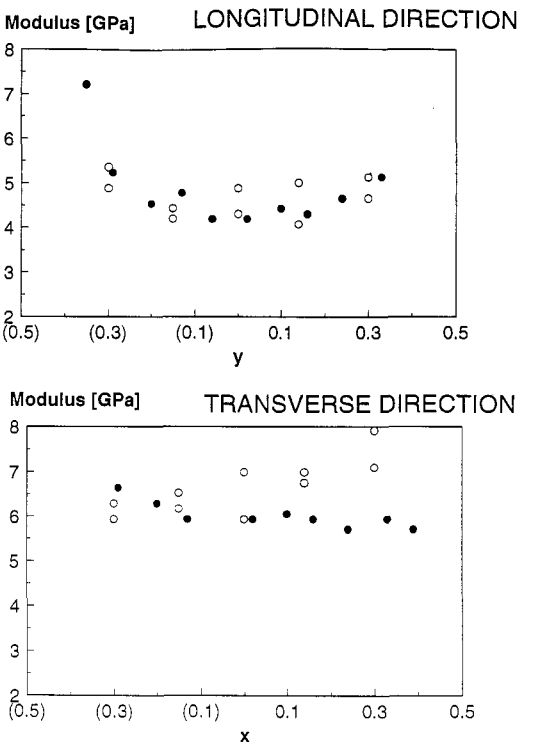

Fig. 14 Creep moduli profile for PP/g - 10 STATIC. for both Figs. open circles are results of the laboratory a, filled-in circles obtained by the laboratory c

Relevant additional information on fibre distribution has been obtained by laboratory c which measured 10 s relaxation moduli of bars prepared by cutting moldeded plaques in both principal directions as indicated in Fig. 5. The results obtained are given in Figs. 13 (Dynamic processing) and 14 (Static injection molding).

The longitudinal moduli for the Dynamic manufacturing clearly depend on the y-coordinate: The value of about 8 GPa is associated with the sides of a molding ($y \rightarrow |Y/2|$), the value at the centre ($y \rightarrow 0$) amounts to 11 GPa. On the other hand, the transverse moduli for the Dynamic injection molding route are position independent with a value around 3.5 GPa.

Concerning the Static injection molding, the longitudinal stiffnesses have a minimum value of 4 GPa near the centre and a maximum value (7 GPa) near the edges ($y \rightarrow |Y/2|$). Once again, the transverse moduli are position (x-coordinate) independent with a mean value of 6 GPa which exceeds the stiffness averaged in the longitudinal direction.

To check whether stiffness profiles have not been induced by different states in the matrix structure, laboratory c also performed relaxation experiments on bars before and after a thermal treatment involving 21 hours annealing at 130 °C and cooling at a rate of about 1 °C/min. As no differences could be observed between annealed and untreated samples, it is concluded that the difference in stiffness values is due to fibre orientation only.

Results generated by laboratory c can be related to the measurements of laboratory a: Using the stiffness profiles contained in Figs. 10 and 11 as the input, stiffness characteristics of the prismatic bars in discrete y and x positions can be synthesised by summing up all the contributions across the thickness Z. An encouraging agreement also shown in Figs. 13 and 14 reflects internal consistency of measurements carried out by laboratories a and c.

Finally, laboratory e studied the through-thickness compressive properties by measuring the yield strength in uniaxial compression. The four types of specimens used and their location in the plaques are described in Fig. 4. The force-displacement curves for these specimens were of two different types as shown in Fig. 15: The type 1 curve is observed for all the specimens originating from the Dynamic mode of processing, whilst the type 2 curve regardless of the sample thickness typifies those moldeded by the Static injection. It is again apparent that the composite's structure influences the deformation process, in this case the compressive yielding. The true uniaxial strength at yielding can be derived in the spirit of eqn. (3) by eliminating frictional contributions as shown in Figs. 16 for the Dynamic processing) and 17 for the Static injection molding. The values of the compressive yield strength σ_y derived from initial intercepts are given in Table 3:

Table 3 Compressive yield strength of the PP/g 10 composite

Processing	Region	Thickness (mm)	σ_y (Mpa)
dynamic		6	40
	core	2	47
	skin	2	70
static		6	10
	core	4	6
	core	2	6
	skin	2	92

All three thicknesses studied for the Dynamic processing mode show higher strength values than the value of 25 MPa characterising the polypropylene matrix. In addition, the 2 mm skin specimens exhibit a higher yield strength than their equivalents from the core region. The results for the Static injection molding are associated with much lower compressive yield values - so low that they are below the matrix characteristic. Presence of voids, likely to result from the 'fountain flow' causing transverse fibre

orientation in the 'core' region, might be a structural, albeit unproved, feature behind this experimental observation.

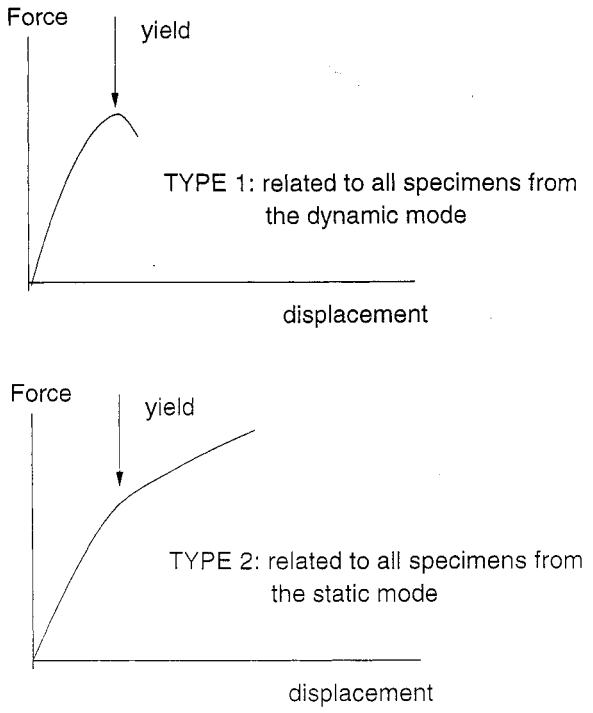

Fig. 15 Typical force-displacement curves for the uniaxial compression test.

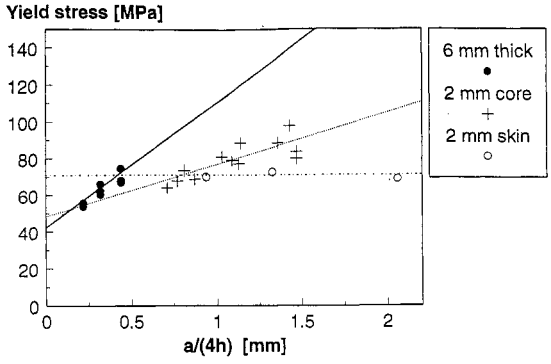

Fig. 16 Uniaxial compressive testing of PP/g - 10 DYNAMIC.

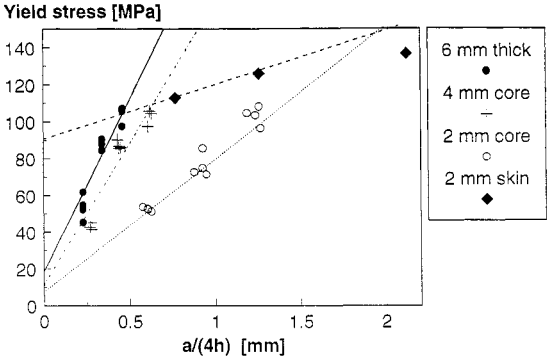

Fig. 17 Uniaxial compressive testing PP/g -10 STATIC.

4. CONCLUSIONS

- Novel experimental approaches, namely determination of the rebound moduli in different directions with respect to a) cutting direction (longitudinal and transverse) and b) wafer orientation (flat- and edge-wise) together with the flexural measurements carried out with circular discs specimens have been used to describe the anisotropy in composite moldings.
- The anisotropy of composite moldings has been found to be governed by the spatial fibre orientation which conforms to a complex pattern in the thickness direction dictated by the processing conditions used during the injection molding.

- The most perfect fibre alignment in the molding direction is attained in the surface (skin) composite layer using Dynamic processing; on the other hand, the classical injection molding (the Static mode) leads to the fibre orientation that is perpendicular to the molding direction in the centre (core) part of the moldings.
- The extreme values of experimentally determined stiffnesses agree with the outcome of the micromechanical modelling. Thus they can be considered to be engineering constants of the lamina reinforced with finite-length fibres and used for further, macromechanical modelling of a more complex structural response.
- Fibre orientation deduced from the mechanical performance correlates well with the outcome of structural studies such as the X-ray crystallography.
- Intrinsic consistency in measurements is indicated by the agreement between properties measured on the whole composite moldings and those synthesised using the information generated on the wafers.
- Finally, fibre orientation in the moldings manufactured by the dynamic and static injection routes conforms to the patterns schematically summarised in Fig. 18.

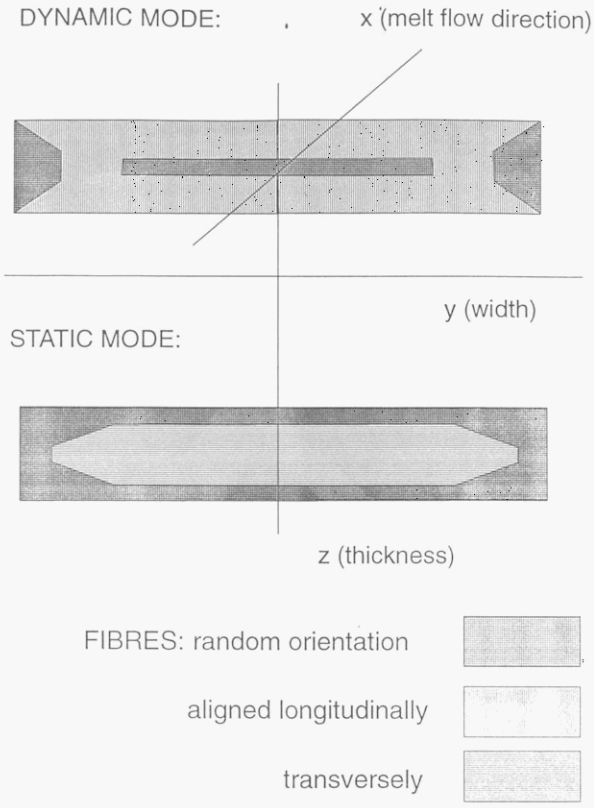

Fig. 18 Structural aspects of moldings deduced from structural evaluation and performance testing.

REFERENCES

1 A. Cervenka & P.S. Allan. Characterization of finite length composites - Part I: Introductory paper, *Pure Appl. Chem.*, 1997, **69**, 1693–1705.

2 L. Glas, P.S. Allan, T. Vu-Khanh & A. Cervenka. Characterization of finite length composites - Part II: Mechanical performance of injection moldeded composites, *Pure Appl. Chem.*1997, **69**, 1707–1723.

3 P.S. Allan, A. Cervenka & D.R. Moore. Characterization of finite length composites - Part V: Modelling of stiffness, *Pure Appl. Chem* 1997, **69**, 1741–1751.

4 G. von Bradsky, R.S. Bailey, A. Cervenka & P.S. Allan. Characterization of finite length composites - Part IV: Determination of structural aspects of composites, *Pure Appl. Chem.*, submitted for publication.

5 T. Casiraghi. *Polym. Eng. Sci* **23**, 16 (1983).

6 T. Casiraghi, G. Castiglioni & L. Colombaroli. unpublished data.

7 R.C. Stephenson, S. Turner & M. Whale. *Polym. Eng. Sci,* **19**, 173 (1979).